

# Effect of antimony substitution in iron pnictide compounds

D. Schmidt<sup>a</sup>, H. F. Braun<sup>a</sup>

<sup>a</sup>*Physikalisches Institut, Lehrstuhl Experimentalphysik V, Universität Bayreuth, 95440 Bayreuth*

## Abstract

In the present study we have examined the effect of negative chemical pressure in iron pnictides. We have synthesized substitution series replacing arsenic by antimony in a number of 1111- and 122-iron arsenides and present their crystallographic and physical properties. The SDW transition temperature in  $\text{LaFeAs}_{1-x}\text{Sb}_x\text{O}$  decreases with increasing antimony content, while the superconducting transition temperature in  $\text{LaFeAs}_{1-x}\text{Sb}_x\text{O}_{0.85}\text{F}_{0.15}$  initially increases with Sb substitution. 1111-compounds with samarium instead of lanthanum have a smaller unit cell volume. In these phases, no Sb solubility is observed. There is also no apparent solubility of antimony in the 122-iron arsenides.

**Keywords:** Fe-based superconductors, powder metallurgy, chemical pressure, electrical transport, X-ray diffraction, phase diagram

## 1. Introduction

The discovery of superconductivity in fluorine doped  $\text{LaFeAsO}$  (1111) compounds [1] was followed by quite a large amount of experimental and theoretical work, which was aimed at understanding the physical properties of iron pnictides. Beside the superconducting 1111 iron pnictides which crystallize in the tetragonal  $\text{ZrCuSiAs}$ -type structure, superconductivity was found in the 122 compounds which crystallize in the  $\text{ThCr}_2\text{Si}_2$  structure type [2] and the 111 compounds with  $\text{PbFCl}$ -type structure [3]. In the present study we concentrate on the 1111-type compounds with formula  $\text{REFeAsO}$  (RE: rare earth) and 122-type compounds with formula  $\text{AEFe}_2\text{As}_2$  (AE: alkaline earth). Both structure types are characterized by layers of  $\text{FeAs}$  which are separated by layers of rare earth oxide or of alkaline earth atoms.

Upon cooling, the undoped compounds undergo a structural phase transition from tetragonal to orthorhombic. Beside this structural transition, there is also a magnetic phase transition to long range antiferromagnetic order. This transition is ascribed to the occurrence of a spin-density-wave (SDW) [4]. In the 122-compounds, the structural and magnetic phase transition takes place at the same temperature whereas in the 1111-compounds the transition temperature of the structural transition is somewhat higher than the magnetic transition temperature [5].

By appropriate doping, it is possible to suppress the SDW and as a consequence superconductivity (SC) may arise. There are several concepts for doping. In the 122-compounds, hole doping on the alkaline earth site by substitution with potassium or sodium results in the highest superconducting transition temperature  $T_c = 38\text{ K}$  for  $\text{Ba}_{0.6}\text{K}_{0.4}\text{Fe}_2\text{As}_2$  [2; 6]. In the 1111-compounds, hole doping can be achieved by substituting the rare earth by an

alkaline earth. For example, the substitution with Sr induces superconductivity with a maximum  $T_c$  of 25 K [7]. In both types of compounds, electron doping was achieved by replacing Fe with e.g. Co [8], Ni [9], Ru [10], Pd or Rh [11] which leads to superconductivity with a maximum  $T_c = 25\text{ K}$  for  $\text{BaFe}_{2-x}\text{Co}_x\text{As}_2$  [12]. By substituting the iron with cobalt in the 1111-compounds, superconductivity was obtained with transition temperatures up to 17 K [13; 14]. These atomic substitutions of an alkaline element for AE, AE for RE or iron by some other transition element of neighbor groups not only changes the electron concentration but at the same time leads to a change in unit cell volume. The effect of such a volume change alone can be observed by the application of hydrostatic pressure.

In both compounds,  $\text{BaFe}_2\text{As}_2$  and  $\text{LaFeAsO}$ , superconductivity can be induced under high pressure, where  $\text{BaFe}_2\text{As}_2$  reaches a maximum  $T_c$  of 29 K at a pressure of 4 GPa [15] while for  $\text{LaFeAsO}$  a maximum  $T_c$  of 21 K is reached at 12 GPa [16].

Similar effects might be obtained by “chemical pressure”, i.e. a change in unit cell volume by isoelectronic substitution on one of the lattice sites. Positive chemical pressure results from the substitution of As through the smaller P. In such substitution the SDW can be suppressed and superconductivity occurs with a maximum  $T_c = 31\text{ K}$  for  $\text{BaFe}_2\text{As}_{1.74}\text{P}_{0.26}$  [17] and up to  $T_c = 11\text{ K}$  for  $\text{LaFeAs}_{1-x}\text{P}_x\text{O}$  ( $x = 0.25 - 0.3$ ) [18].

The possible substitution of Sb for As, corresponding to negative chemical pressure, has been examined in theoretical studies. First principle calculations were performed by density-functional methods on compounds which had not been synthesized then. In the 1111-compounds the substitution was predicted to cause an enhanced Fermi surface nesting and the 1111-compound with antimony is described as a candidate for higher  $T_c$  values [19]. In

the 122-compounds no enhanced nesting is predicted [20]. For both the 1111- and 122-compounds with antimony, expected lattice parameters have been calculated [19; 20; 21].

Experimentally, it was possible to substitute the As by Sb in the LaFeOAs compounds. With increasing Sb content, there is a decrease of the SDW and structural phase transition temperature, however, no superconductivity is induced [22]. To complement the investigations on the fluorine free 1111-compounds we have synthesized both the lanthanum and samarium compounds.

Wang et al. reported on Sb substitution in fluorine doped 1111-samples and found a recovery of the SDW transition in  $\text{LaFeAs}_{1-x}\text{Sb}_x\text{O}_{0.9}\text{F}_{0.1}$  with  $x > 0.1$  [23]. In order to expand the phase diagram of the fluorine doped system, we prepare an antimony substitution series with a fluorine content of 0.15. So far, to the best of our knowledge, there are no experimental results available about the possibility of Sb substitution in  $\text{BaFe}_2\text{As}_2$ . In order to compare the 1111- and 122-compounds with respect to the influence of Sb substitution on the SDW transition as well as on the superconducting transition we used non-superconducting  $\text{BaFe}_2\text{As}_2$  and superconducting  $\text{BaFe}_{1.83}\text{Co}_{0.17}\text{As}_2$  as parent compounds for our Sb substitution experiments with the 122-compounds.

## 2. Materials and Methods

Due to the air sensitivity of the Ba-containing precursor, all preparation steps were carried out in a glove box filled with dry Ar-gas. The synthesis of the polycrystalline samples was carried out in sealed quartz glass tubes under inert atmosphere, by solid state reaction of the precursors BaAs,  $\text{Fe}_2\text{As}$  (Alfa Aesar 99.5 %),  $\text{Co}_2\text{As}$  and  $\text{Fe}_2\text{Sb}$ , respectively. The precursor BaAs was synthesized by a vapour transport method. It was important that Ba and As were not in direct contact since their highly exothermic reaction lead to a rapid increase of vapour pressure, even at moderate temperature, which could break the quartz tube.

To avoid such uncontrolled reactions, Ba chunks (Alfa Aesar 99.2 %) were kept in a corundum crucible inside a quartz glass container while As pellets (Alfa Aesar 99.99 %) in a 1:1 molar ratio were placed underneath or around this crucible. The tube was evacuated, sealed under Ar at a pressure of 0.05 bar and heated up slowly in a box-type furnace to 973 K. This temperature was kept for 5 d. After the heat treatment, the As had evaporated and quantitatively reacted with the Ba. The reaction results in dark grey lumps with mean composition BaAs. The  $\text{Co}_2\text{As}$  and  $\text{Fe}_2\text{As}$  precursors were prepared by slowly heating stoichiometric mixtures of the elements (Fe powder Grüssing 99.9 %, Co powder Alfa Aesar 99.8 %, Sb shot Alfa Aesar 99.9999 %) and keeping them at 973 K for 48 h in an evacuated quartz capsule. In order to synthesize the substitution series, the precursors were ground, mixed together in the appropriate ratio, pressed into pellets and

heated at a rate of  $100\text{ K h}^{-1}$  up to 1123 K under Ar atmosphere. After the 48 h treatment, dark grey pellets were obtained which are reasonably stable in air.

Polycrystalline samples of 1111 compounds were obtained by solid state reaction of the stoichiometric mixture of REAs (RE: La, Sm), RESb,  $\text{Fe}_2\text{O}_3$ ,  $\text{REF}_3$  and Fe powders. The mixture was prepared in an Ar filled glove-box, pressed into pellets, sealed in quartz tubes with an Ar pressure of 0.05 bar and heated in a box-type furnace with a rate of  $50\text{ K h}^{-1}$  to 1373 K. After 48 h the furnace was switched off and cooled down to room temperature. After the heat treatment dark grey pellets were obtained, which are reasonably stable in air. The rare-earth arsenide and antimonide precursors were prepared by heat treatment of a stoichiometric mixture of the elements at 670 K for 12 h in an evacuated quartz tube.

The samples were characterized at room temperature by X-ray powder diffraction using a Seifert XRD 3000 diffractometer in Bragg-Brentano geometry with  $\text{CuK}_\alpha$  radiation and secondary Ge(002) monochromator. Data was collected from  $10^\circ$  -  $100^\circ$  in steps of  $0.02^\circ$ . To determine the lattice parameters and the atomic positions, we used the LeBail method and Rietveld refinement, respectively. Crystal quality was tested by SEM/EDX using a Zeiss LEO 1530 (FE-SEM with Schottky-field-emission cathode, in-lens detector, Back Scattered Electron Detector) using an accelerating voltage of 10 kV. The EDX data was collected by an INCA Energy System from Oxford Instruments. The temperature dependence of dc resistivity was measured with a standard four probe technique. Small rods with a length of 5 mm and thickness of 1 mm were cut from the pellets and four copper wires were connected with conductive silver. To confirm the occurrence of superconductivity, we used a home made magnetic susceptibility meter and measured the screening signal at a frequency of 2.7 kHz.

## 3. Results

### *Ba122 samples*

The powder patterns of non-superconducting cobalt-free samples with composition  $\text{BaFe}_2\text{As}_{2-x}\text{Sb}_x$  could be well indexed with the tetragonal  $\text{ThCr}_2\text{Si}_2$ -type structure of space-group  $I4/mmm$ . The lattice parameters of the Sb-free samples  $a = 3.9623(2)\text{ \AA}$  and  $c = 13.024(1)\text{ \AA}$  agree with the results published by Rotter et al. [4] and, judged from powder X-ray results, the samples are single-phase. For the antimony free sample we obtain a residual from Rietveld refinement of  $R_p = 4.49\%$ . The lattice parameters and unit cell volume versus nominal Sb concentration of the substitution series are plotted in Fig. 1. A slight increase of the lattice parameters with  $x$  is suggested, however, this increase is smaller than the standard deviation of the measured values and thus cannot be taken as evidence for the solubility of antimony in this structure. In order to confirm this, we released the occupation numbers

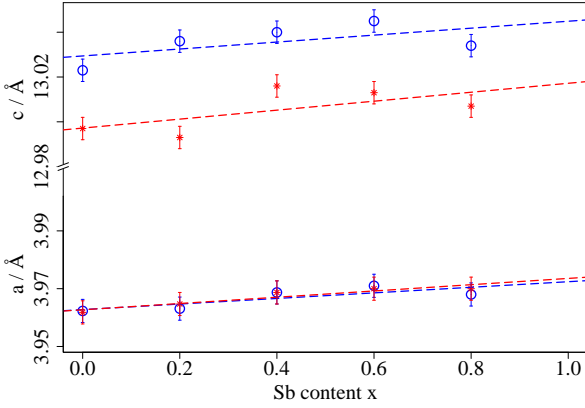


Figure 1: Lattice parameters versus Sb content in  $\text{BaFe}_{2-y}\text{Co}_y\text{As}_{2-x}\text{Sb}_x$ . Blue: non-superconducting samples ( $y = 0$ ) with SDW-transition; Red: superconducting compounds ( $y = 0.17$ ). The tiny trend of increasing lattice parameters is within the standard deviation errors and therefore no proof for a successful Sb substitution in the 122-compounds.

of arsenic and antimony in the refinement. For the  $x = 0$  and  $x = 0.4$  samples we found no occupation of antimony at the arsenic site. There is an increase of the residual to  $R_p = 10.47\%$  at  $x = 0.4$ . In the qualitative phase analysis we found impurity phases up to an impurity level of 20 %. We were able to identify iron arsenide and iron antimonide as well as barium silicate which appears to be a reaction product of the alkaline earth with the quartz glass ampoule.

The temperature dependent measurement of resistivity down to 4.2 K for the antimony free sample reveals a transition at 136(5) K related to the SDW transition. This transition temperature is not affected by increasing the nominal antimony concentration.

The powder patterns of the Co-substituted superconducting samples  $\text{BaFe}_{1.83}\text{Co}_{0.17}\text{As}_{2-x}\text{Sb}_x$  could also be indexed with the  $\text{ThCr}_2\text{Si}_2$ -type structure. The antimony free sample had also a single phase X-ray pattern. The lattice parameters of the antimony free sample are  $a = 3.9618(2) \text{ \AA}$  and  $c = 12.997(1) \text{ \AA}$ , slightly smaller than the parameters of the non-superconducting  $x = 0$  sample, indicative of a successful cobalt substitution. The residual is  $R_p = 6.77\%$ . The lattice parameters of samples with higher nominal antimony content remain unchanged within standard deviation errors. However, impurity phases appear in the powder patterns and there is also an increase of the residual.

The temperature dependent electrical resistivity down to 4.2 K shows a drop to zero at  $T_c = 24 \text{ K}$ . The appearance of superconductivity was confirmed by measuring the screening signal in ac-susceptibility, which confirmed the transition temperature, in good agreement with literature [4; 24]. With higher nominal antimony concentrations we found no change in transition temperatures neither in the Co-free SDW samples, nor in the Co-substituted super-

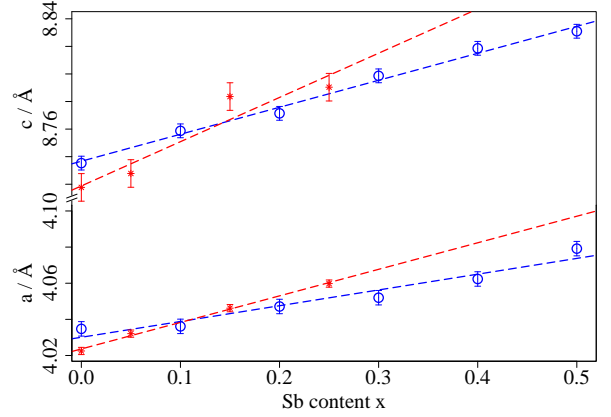


Figure 2: Lattice parameters of  $\text{LaFeAs}_{1-x}\text{Sb}_x\text{O}_{1-y}\text{F}_y$  versus the nominal antimony content. Blue: Non-superconducting ( $y = 0$ ) compounds; Red: superconducting ( $y = 0.15$ ) compounds. The parameters follow Vegard's law (see eqns. 1–4). For the non-superconducting compounds the limit of solubility lies at  $x = 0.5$  and for the superconducting compounds at  $x = 0.25$ .

conducting samples.

#### La1111 samples

In figure 2 the variation of the lattice parameters with antimony content is shown. Shown in blue are the results for the  $\text{LaFeAs}_{1-x}\text{Sb}_x\text{O}$  series with SDW character and in red for the superconducting  $\text{LaFeAs}_{1-x}\text{Sb}_x\text{O}_{0.85}\text{F}_{0.15}$  samples. At room temperature, the diffraction patterns could be well indexed by a tetragonal  $\text{ZrCuSiAs}$  structure with space group  $P4/\text{mmm}$ .

The  $R_p$  factor for the non-superconducting antimony free sample was determined to 4.66 %, indicative for a single phase sample. The lattice parameters were  $a = 4.0348(1) \text{ \AA}$  and  $c = 8.7362(4) \text{ \AA}$ . The lattice parameters increase with increasing antimony content following Vegard's law between an antimony content of 0 and 0.5 with:

$$a = [0.087(11) \cdot x + 4.040(3)] \text{ \AA} \quad (1)$$

$$c = [0.196(10) \cdot x + 8.737(3)] \text{ \AA} \quad (2)$$

For higher nominal antimony concentrations  $x > 0.5$ , no homogeneous samples were obtained. The lattice parameters of the  $\text{ZrCuSiAs}$ -type phase do not increase further, instead, impurity phases appear.

The  $R_p$  factor of the antimony free superconducting sample is 6.39 %, the lattice parameters are  $a = 4.0225(1) \text{ \AA}$  and  $c = 8.7177(4) \text{ \AA}$ . Between an antimony content of 0 and 0.25 the lattice parameters follow Vegard's law, well described by:

$$a = [0.146(7) \cdot x + 4.023(1)] \text{ \AA} \quad (3)$$

$$c = [0.32(7) \cdot x + 8.72(1)] \text{ \AA} \quad (4)$$

For higher nominal antimony concentrations  $x > 0.25$ , no homogeneous samples were obtained.

The non-superconducting samples show two transitions in the resistivity signal similar to those described in [5].

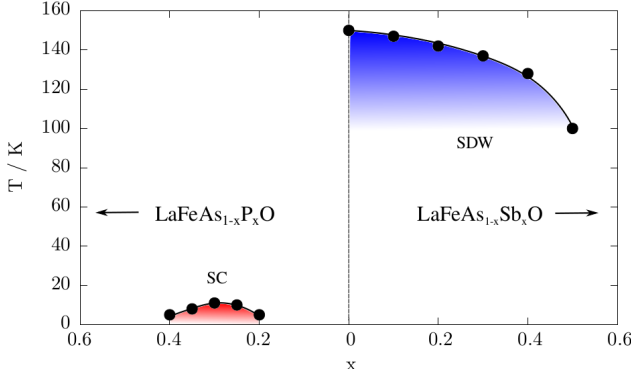


Figure 3: Right: Mean value of the crystallographic/SDW transition (see text) versus antimony content  $x$ . The part shaded in blue shows the temperatures measured in the present work. No superconductivity was found down to 4.2 K. Left: The red part shows the superconducting regime of phosphorus doped compounds, taken from [18].

The first transition refers to the structural phase transition from a tetragonal to an orthorhombic structure. For the  $x = 0$  sample we found the transition temperature  $T_S = 160$  K. The second transition refers to the Néel temperature  $T_N = 135$  K. The temperature difference between the structural and magnetic transition is constant over the investigated antimony range, thus, for the sake of simplicity, we plot the mean of the transition temperatures  $(T_S + T_N)/2$  in figure 3, labelled SDW and emphasized by blue color. With higher antimony concentration, the transition temperatures decrease. Within the homogeneous range we found a minimum mean transition temperature of 100 K for  $x = 0.5$  but no superconductivity down to 4.2 K. For higher Sb concentration, the semiconducting behaviour of impurities dominates the resistivity signal and it became impossible to extract transition temperatures for the LaFeAsO phase.

With a fluorine content of  $y = 0.15$ , the samples are superconducting. For Sb-free samples we found a transition temperature of  $T_c = 9$  K which agrees with the phase diagram suggested in Oka et al. [25]. With increasing antimony content, the transition temperature increases up to a maximum  $T_c$  of 28 K in the resistivity signal and 25 K in the ac susceptibility signal. The black data points in figure 4 show the mean transition temperature of our resistivity and susceptibility measurements. The additional points plotted in green and in blue are taken from Wang et al. [23].

#### Sm1111 samples

When lanthanum is replaced with samarium, the cell volume of the 1111 phase is smaller. We measured  $a = 3.939(5)$  Å and  $c = 8.49(1)$  Å in good agreement with [26]. However, with increasing nominal antimony content, merely the impurity level increases and the crystallographic and physical properties of the 1111 phase remain constant. Thus, we conclude that there is no solubility of antimony in SmFeAs<sub>1-x</sub>Sb<sub>x</sub>O.

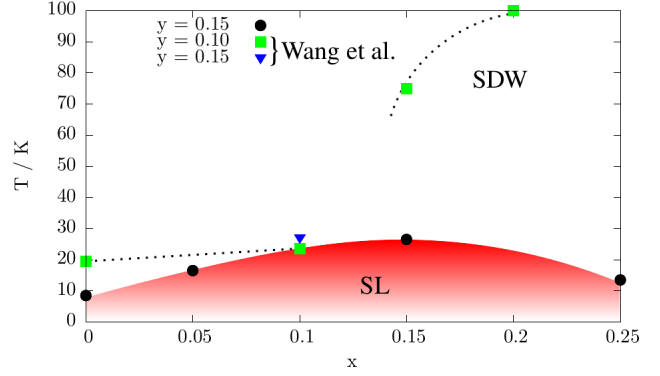


Figure 4: Mean superconducting transition temperatures of LaFeAs<sub>1-x</sub>Sb<sub>x</sub>O<sub>1-y</sub>F<sub>y</sub> with  $y = 0.15$  versus antimony content  $x$  (black points). We find a maximum  $T_c$  of 26.5 K in this system and no SDW transition. Squares (plotted in green) and triangles (in blue) are taken from Wang et al. [23]

#### 4. Discussion

The invariance of the crystallographic and physical properties in the 122-compounds against nominal Sb concentration as well as direct structure refinements prove the absence of solubility of Sb in this structure. BaFe<sub>2</sub>As<sub>2</sub> has the highest unit cell volume in the class of known 122 iron arsenides. It is thus unlikely that Sb can be substituted into 122 iron pnictide compounds with smaller unit cell volume. The unit cell size of BaFe<sub>2</sub>As<sub>2</sub> appears to be at the stability limit of this class of compounds.

The measured lattice parameters of the non-superconducting La1111 parent compounds agree well with the values computed in [21] or [19]. However, the slope of the linear regression with Vegard's law differs from the measured data. In [21] the slope of  $a$  is 0.1271 Å and 0.6078 Å for  $c$  and in [19] it is 0.107 Å for  $a$  and 0.551 Å for  $c$ . Our smaller slope of 0.087 Å for  $a$  and 0.196 Å for  $c$  may be a result of increasing disorder which was neglected in the calculation of the lattice parameters in the theoretical studies. We find that La1111 compounds show a solubility up to an antimony concentration of  $x = 0.5$  in the non-superconducting compounds confirming [22] and  $x = 0.25$  in the superconducting fluorine doped compounds with  $y = 0.15$ . Carlsson et al. found slightly larger lattice parameter for the non-superconducting Sb-substituted compounds but the same trend in the SDW transition temperature [22]. With increasing lattice parameters, that is negative chemical pressure, the interlayer distance between the FeAs layers increases due to the larger  $c$  axis and thus the magnetic interaction is weakened. As a consequence, the SDW transition temperature decreases from 150 K for  $x = 0$  to 100 K for  $x = 0.5$ .

With higher antimony concentration, no single phase samples were obtained. We conclude that there is a solubility limit for antimony near  $x = 0.5$ . In contrast to the phosphorus substituted compounds [18], we found no superconductivity in the antimony substituted compounds, in agreement with [22]. The SDW cannot be suppressed

and superconductivity cannot emerge because of the enhanced Hund's rule coupling discussed in [19]. The Fe  $d$  states are localized since the orbital overlap is reduced due to the larger iron-pnictogen distance.

The results on the fluorine doped samples reveal an increase of the superconducting transition temperature with increasing Sb concentration. A problem is the exact determination of fluorine content. We have compared the transition temperature of our  $x = 0$  compound with the phase diagram from [25] and find agreement with the 0.15 fluorine doping level. Another benchmark is the point for  $x = 0.1, y = 0.15$  from [23] which agrees with our suggested phase diagram (blue triangle in Fig. 4). With our compounds and measurement techniques, we found a maximum  $T_c$  of 27 K in the  $\text{LaFeAs}_{1-x}\text{Sb}_x\text{O}_{0.85}\text{F}_{0.15}$  system. In contrast to the work of Wang et al. (green squares in Fig. 4), we found no recurrence of the SDW transition with higher antimony content. For concentrations higher than  $x = 0.25$  we obtain no single phase compounds.

The smaller unit cell volume of the samarium compounds leads to a blockade of solubility of antimony. We found no variation of crystallographic and physical properties with nominal antimony content. Obviously, there is no solubility of antimony in the  $\text{Sm1111}$ -system.

## 5. Conclusion

We have investigated the solubility of Sb in some iron arsenides of the 122 and 1111 type. In the case of fluorine-free  $\text{LaFeAs}_{1-x}\text{Sb}_x\text{O}$  compounds, the substitution was possible up to a solubility limit  $x = 0.5$ . The SDW transition temperature decreases with increasing Sb concentration. The solubility limit of Sb in the superconducting fluorine-doped compounds  $\text{LaFeAs}_{1-x}\text{Sb}_x\text{O}_{0.85}\text{F}_{0.15}$  is  $x = 0.25$ . We found a maximum  $T_c$  of 27 K at  $x = 0.15$ . No antimony substitution of arsenic was possible in the  $\text{Sm1111}$  and the  $\text{Ba122}$  compounds. With the application of "negative chemical pressure", these compounds become unstable against the formation of foreign phases.

## Acknowledgements

We thank M. Heider from the "Bayreuther Institut für Makromolekülforschung" for the SEM/EDX measurements. N. Kurz, L. Wehmeier and S. Wolf for their help with sample preparation and last but not least C. Kerling for the technical support in our lab.

## References

- [1] Y. Kamihara, T. Watanabe, M. Hirano, H. Hosono, Iron-based layered superconductor  $\text{LaO}_{1-x}\text{F}_x\text{FeAs}$  ( $x = 0.05$ -0.12) with  $T_c = 26$  K, *Journal of the American Chemical Society* 130 (11) (2008) 3296–3297. doi:10.1021/ja800073m.
- [2] M. Rotter, M. Tegel, D. Johrendt, Superconductivity at 38 K in the iron arsenide  $\text{Ba}_{1-x}\text{K}_x\text{Fe}_2\text{As}_2$ , *Physical Review Letters* 101 (10) (2008) 1070064. doi:10.1103/PhysRevLett.101.107006.
- [3] J. H. Tapp, Z. Tang, B. Lv, K. Sasmal, B. Lorenz, P. C. W. Chu, A. M. Guloy,  $\text{LiFeAs}$ : An intrinsic FeAs-based superconductor with  $T_c=18$  K, *Physical Review B* 78 (6) (2008) 060505. doi:10.1103/PhysRevB.78.060505.
- [4] M. Rotter, M. Tegel, D. Johrendt, I. Schellenberg, W. Hermes, R. Pöttgen, Spin-density-wave anomaly at 140 K in the ternary iron arsenide  $\text{BaFe}_2\text{As}_2$ , *Physical Review B* 78 (2) (2008) 020503. doi:10.1103/PhysRevB.78.020503.
- [5] H.-H. Klauss, H. Luetkens, R. Klingeler, C. Hess, F. J. Litterst, M. Kraken, M. M. Korshunov, I. Eremin, S.-L. Drechsler, R. Khasanov, A. Amato, J. Hamann-Borrero, N. Leps, A. Kondrat, G. Behr, J. Werner, B. Büchner, Commensurate Spin Density Wave in  $\text{LaFeAsO}$ : A Local Probe Study, *Physical Review Letters* 101 (7) (2008) 077005. doi:10.1103/PhysRevLett.101.077005.
- [6] S. Aswartham, M. Abdel-Hafiez, D. Bombor, M. Kumar, A. U. B. Wolter, C. Hess, D. V. Evtushinsky, V. B. Zabolotnyy, A. A. Kordyuk, T. K. Kim, S. V. Borisenko, G. Behr, B. Büchner, S. Wurmehl, Hole doping in  $\text{BaFe}_2\text{As}_2$ : The case of  $\text{Ba}_{1-x}\text{Na}_x\text{Fe}_2\text{As}_2$  single crystals, *Physical Review B* 85 (22) (2012) 224520. doi:10.1103/PhysRevB.85.224520.
- [7] H.-H. Wen, G. Mu, L. Fang, H. Yang, X. Zhu, Superconductivity at 25 K in hole-doped  $\text{La}_{1-x}\text{Sr}_x\text{OFeAs}$ , *EPL (Europhysics Letters)* 82 (1) (2008) 17009. doi:10.1209/0295-5075/82/17009.
- [8] A. S. Sefat, R. Jin, M. A. McGuire, B. C. Sales, D. J. Singh, D. Mandrus, Superconductivity at 22 K in Co-doped  $\text{BaFe}_2\text{As}_2$  crystals, *Phys. Rev. Lett.* 101 (11) (2008) 117004. doi:10.1103/PhysRevLett.101.117004.
- [9] A. S. Sefat, M. A. McGuire, R. Jin, B. C. Sales, D. Mandrus, F. Ronning, E. D. Bauer, Y. Mozharivskij, Structure and anisotropic properties of  $\text{BaFe}_{2-x}\text{Ni}_x\text{As}_2$  ( $x=0,1$  and 2) single crystals, *Physical Review B* 79 (9) (2009) 094508. doi:10.1103/PhysRevB.79.094508.
- [10] S. Sharma, A. Bharathi, S. Chandra, V. R. Reddy, S. Paulraj, A. T. Satya, V. S. Sastry, A. Gupta, C. S. Sundar, Superconductivity in Ru-substituted polycrystalline  $\text{BaFe}_{2-x}\text{Ru}_x\text{As}_2$ , *Physical Review B* 81 (17) (2010) 174512. doi:10.1103/PhysRevB.81.174512.
- [11] N. Ni, A. Thaler, A. Kracher, J. Q. Yan, S. L. Bud'ko, P. C. Canfield, Phase diagrams of  $\text{Ba}(\text{Fe}_{1-x}\text{Mn}_x)_2\text{As}_2$  single crystals ( $M = \text{Rh}$  and  $\text{Pd}$ ), *Physical Review B* 80 (2) (2009) 024511. doi:10.1103/PhysRevB.80.024511.
- [12] X. F. Wang, T. Wu, G. Wu, R. H. Liu, H. Chen, Y. L. Xie, X. H. Chen, The peculiar physical properties and phase diagram of  $\text{BaFe}_{2-x}\text{Co}_x\text{As}_2$  single crystals, *New Journal of Physics* 11 (4) (2009) 045003. doi:10.1088/1367-2630/11/4/045003.
- [13] A. S. Sefat, A. Huq, M. A. McGuire, R. Jin, B. C. Sales, D. Mandrus, L. M. D. Cranswick, P. W. Stephens, K. H. Stone, Superconductivity in  $\text{LaFe}_{1-x}\text{Co}_x\text{AsO}$ , *Physical Review B* 78 (10) (2008) 104505. doi:10.1103/PhysRevB.78.104505.
- [14] C. Wang, Y. K. Li, Z. W. Zhu, S. Jiang, X. Lin, Y. K. Luo, S. Chi, L. J. Li, Z. Ren, M. He, H. Chen, Y. T. Wang, Q. Tao, G. H. Cao, Z. A. Xu, Effects of cobalt doping and phase diagrams of  $\text{LFe}_{1-x}\text{Co}_x\text{AsO}$  ( $L = \text{La}$  and  $\text{Sm}$ ), *Physical Review B* 79 (5) (2009) 054521. doi:10.1103/PhysRevB.79.054521.
- [15] P. L. Alireza, Y. T. C. Ko, J. Gillett, C. M. Petrone, J. M. Cole, G. G. Lonzarich, S. E. Sebastian, Superconductivity up to 29 K in  $\text{SrFe}_2\text{As}_2$  and  $\text{BaFe}_2\text{As}_2$  at high pressures, *Journal of Physics: Condensed Matter* 21 (1) (2009) 012208.
- [16] H. Okada, K. Igawa, H. Takahashi, Y. Kamihara, M. Hirano, H. Hosono, K. Matsubayashi, Y. Uwatoko, Superconductivity under High Pressure in  $\text{LaFeAsO}$ , *Journal of the Physical Society of Japan* 77 (11) (2008) 113712. doi:10.1143/JPSJ.77.113712.
- [17] S. Kasahara, T. Shibauchi, K. Hashimoto, K. Ikada, S. Tonegawa, R. Okazaki, H. Shishido, H. Ikeda, H. Takeya, K. Hirata, T. Terashima, Y. Matsuda, Evolution from non-Fermi to Fermi-liquid transport via isovalent doping in  $\text{BaFe}_2(\text{As}_{1-x}\text{P}_x)_2$  superconductors, *Physical Review B* 81 (18) (2010) 184519. doi:10.1103/PhysRevB.81.184519.

- [18] C. Wang, S. Jiang, Q. Tao, Z. Ren, Y. Li, L. Li, C. Feng, J. Dai, G. Cao, Z.-A. Xu, Superconductivity in  $\text{LaFeAs}_{1-x}\text{P}_x\text{O}$ : Effect of chemical pressures and bond covalency, *EPL (Europhysics Letters)* 86 (4) (2009) 47002. doi:10.1209/0295-5075/86/47002.
- [19] C.-Y. Moon, S. Y. Park, H. J. Choi, Enhanced spin-density wave in  $\text{LaFeSbO}$  from first principles, *Physical Review B* 78 (21) (2008) 212507. doi:10.1103/PhysRevB.78.212507.
- [20] C.-Y. Moon, S. Y. Park, H. J. Choi, Dominant role of local-moment interactions in the magnetic ordering of iron pnictide superconductors: A comparative study of arsenides and antimonides from first principles, *Physical Review B* 80 (5) (2009) 054522. doi:10.1103/PhysRevB.80.054522.
- [21] S. Lebègue, Z. P. Yin, W. E. Pickett, The delicate electronic and magnetic structure of the  $\text{LaFePnO}$  system ( $\text{Pn} = \text{pnictogen}$ ), *New Journal of Physics* 11 (2) (2009) 025004. doi:10.1088/1367-2630/11/2/025004.
- [22] S. J. E. Carlsson, F. Levy-Bertrand, C. Marcenat, A. Sulpice, J. Marcus, S. Pairis, T. Klein, M. Nez-Regueiro, G. Garbarino, T. Hansen, V. Nassif, P. Toulemonde, Effect of the isoelectronic substitution of Sb for As on the magnetic and structural properties of  $\text{LaFeAs}_{1-x}\text{Sb}_x\text{O}$ , *Physical Review B* 84 (10) (2011) 104523. doi:10.1103/PhysRevB.84.104523.
- [23] C. Wang, Z. Ma, S. Jiang, Y. Li, Z.-A. Xu, G. Cao, Structural and superconducting properties in  $\text{LaFeAs}_{1-x}\text{Sb}_x\text{O}_{1-y}\text{F}_y$ , *Science China Physics, Mechanics and Astronomy* 53 (7) (2010) 1225–1229, arXiv: 1004.2940. doi:10.1007/s11433-010-0197-8.
- [24] Y. Nakajima, T. Taen, T. Tamegai, Possible Superconductivity above 25 K in Single-Crystalline Co-Doped  $\text{BaFe}_2\text{As}_2$ , *Journal of the Physical Society of Japan* 78 (2) (2009) 023702. doi:10.1143/JPSJ.78.023702.
- [25] T. Oka, Z. Li, S. Kawasaki, G. F. Chen, N. L. Wang, G.-Q. Zheng, Antiferromagnetic Spin Fluctuations above the Dome-Shaped and Full-Gap Superconducting States of  $\text{LaFeAsO}_{1-x}\text{F}_x$  Revealed by  $^{75}\text{As}$ -Nuclear Quadrupole Resonance, *Physical Review Letters* 108 (4) (2012) 047001. doi:10.1103/PhysRevLett.108.047001.
- [26] X. H. Chen, T. Wu, G. Wu, R. H. Liu, H. Chen, D. F. Fang, Superconductivity at 43K in  $\text{SmFeAsO}_{1-x}\text{F}_x$ , *Nature* 453 (7196) (2008) 761–762. doi:10.1038/nature07045.